

Supplementary Information

Arabidopsis TRB proteins function in H3K4me3 demethylation by recruiting JMJ14.

Ming Wang^{1*}, Zhenhui Zhong^{1*}, Javier Gallego-Bartolomé^{1,7}, Suhua Feng^{1,2}, Yuan-Hsin Shih^{1,3}, Mukun Liu¹, Jessica Zhou¹, John Curtis Richey¹, Charmaine Ng¹, Yasaman Jami-Alahmadi⁴, James Wohlschlegel⁴, Keqiang Wu³, and Steven E. Jacobsen^{1,2,4,5,6}.

¹Department of Molecular, Cell and Developmental Biology, University of California at Los Angeles, Los Angeles, CA 90095, USA

²Eli & Edythe Broad Center of Regenerative Medicine & Stem Cell Research, University of California at Los Angeles, Los Angeles, CA 90095, USA

³Institute of Plant Biology, National Taiwan University, Taipei, 10617 Taiwan

⁴Department of Biological Chemistry, University of California at Los Angeles, CA 90095, USA

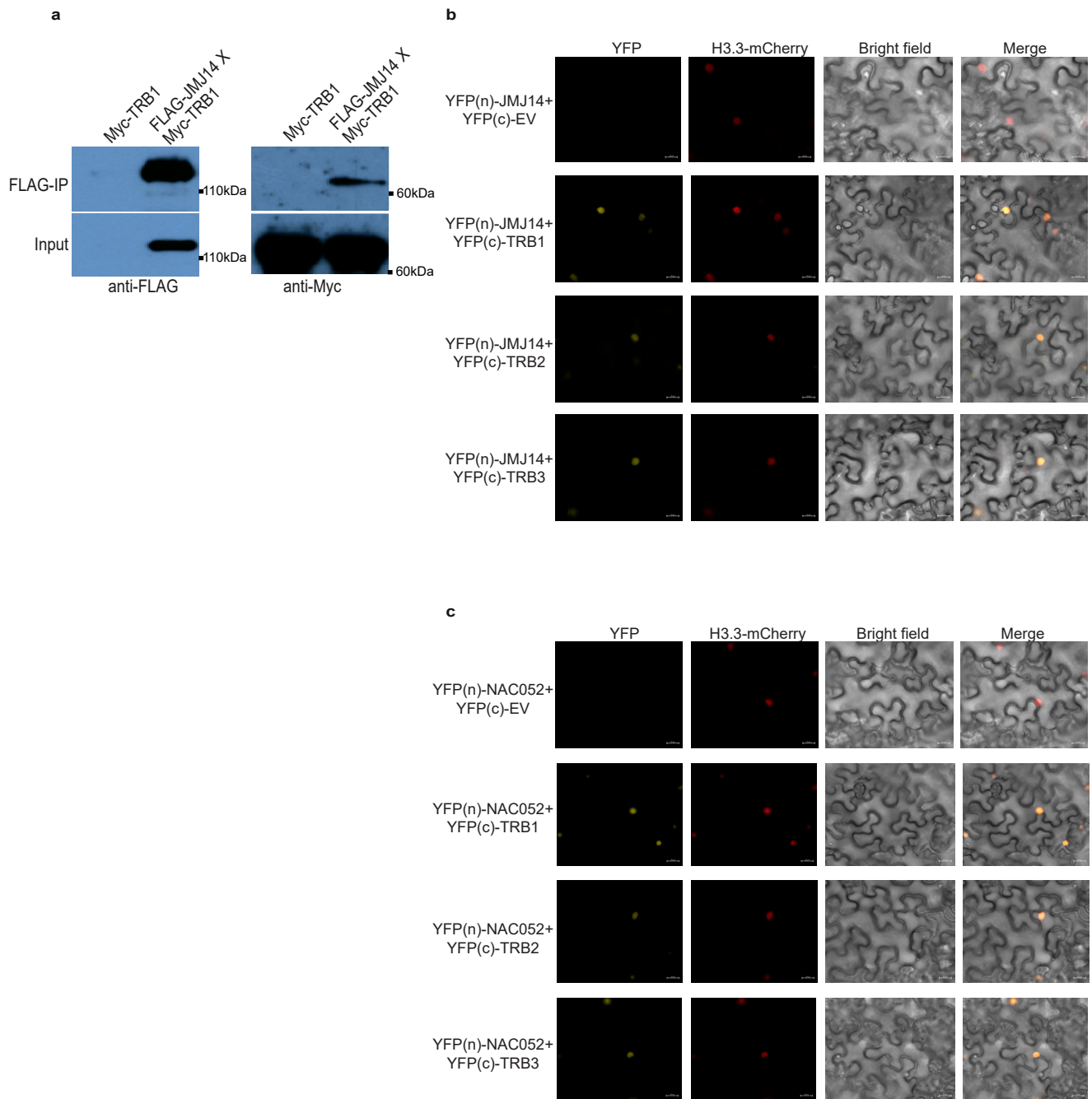
⁵Howard Hughes Medical Institute (HHMI), University of California at Los Angeles, Los Angeles, CA 90095, USA

⁶Correspondence: jacobsen@ucla.edu

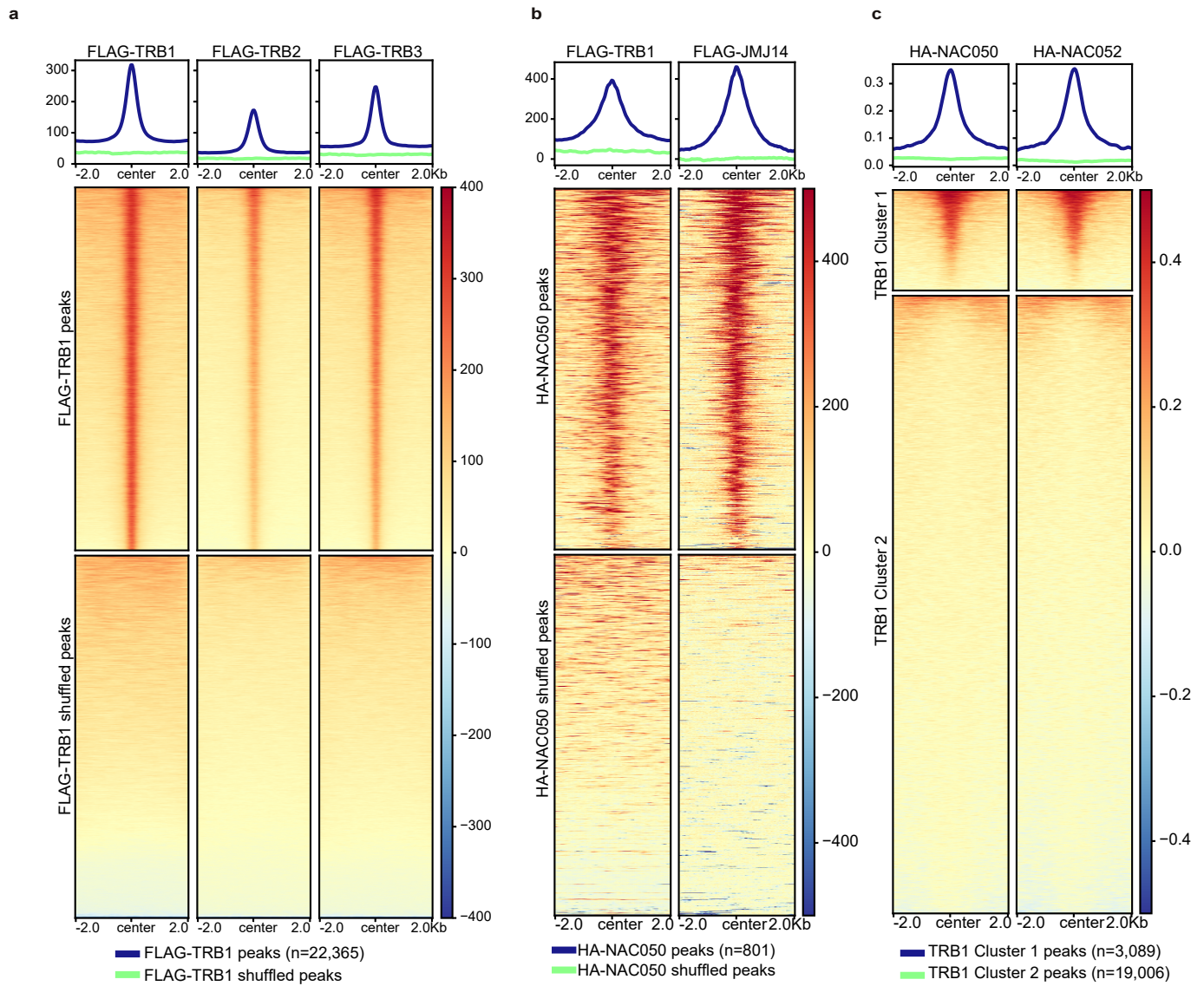
⁷Present address: Instituto de Biología Molecular y Celular de Plantas (IBMCP), CSIC-Universitat Politècnica de València, 46022 Valencia, Spain

*These authors contributed equally

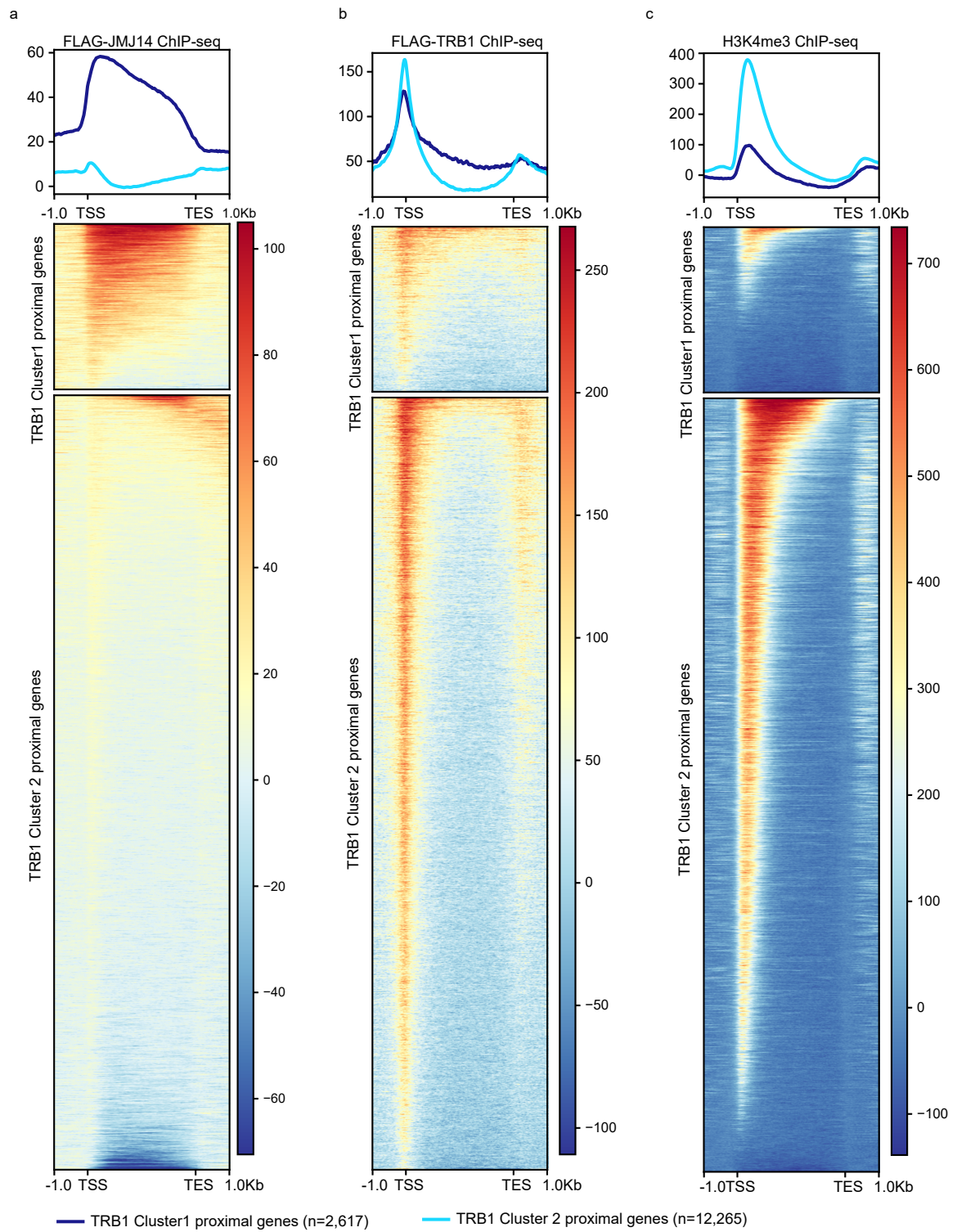
Supplementary Figs. 1-18



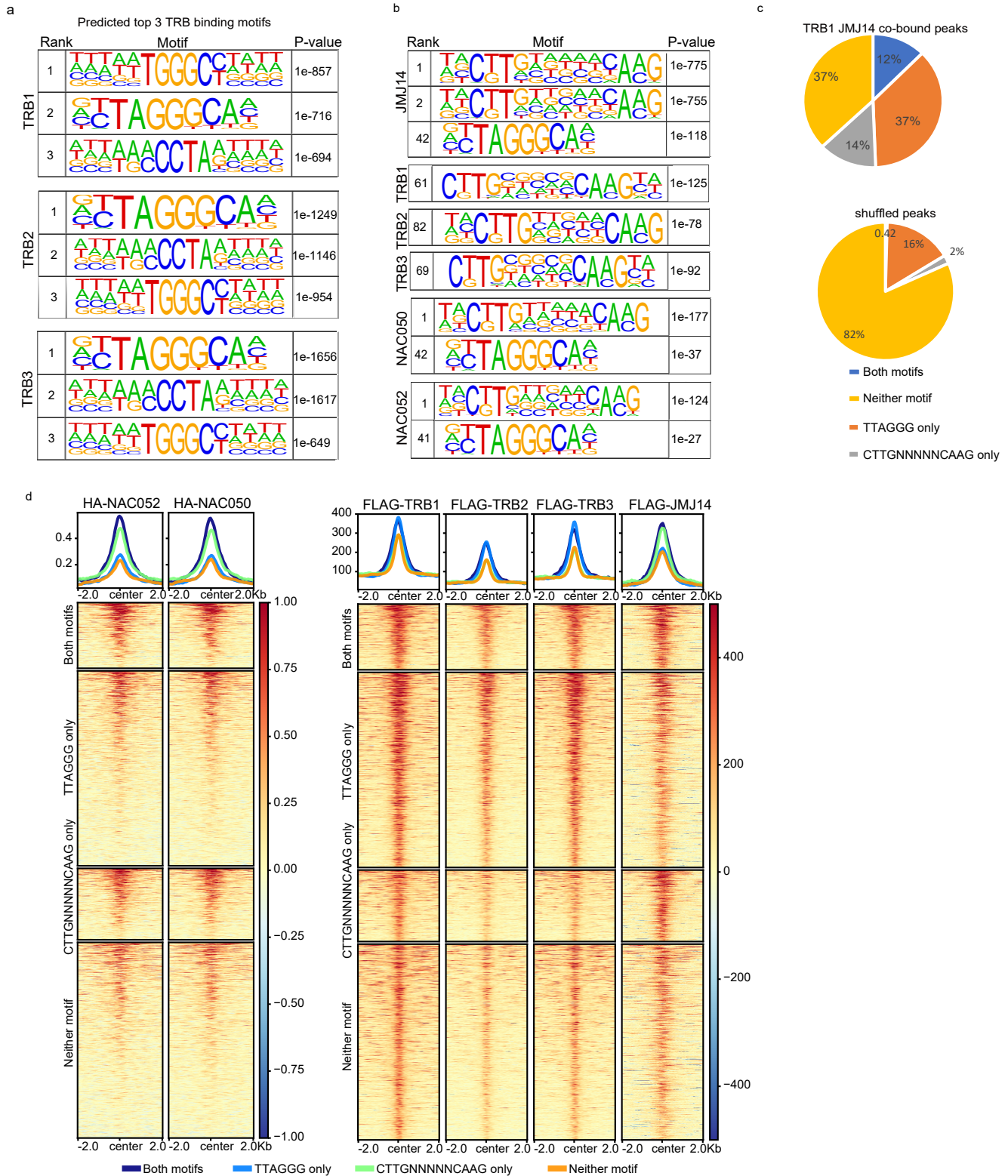
Supplementary Fig. 1 FLAG-TRB1 interacts with Myc-JMJ14. **a** Western blot showing the Co-immunoprecipitation (Co-IP) assay in FLAG-JMJ14 and Myc-TRB1 F2 crossed lines. **b-c** BiFC assays showing the YFP signals of leaves transiently co-expressing cYFP-TRBs and nYFP-JMJ14 (**b**) or nYFP-NAC052 (**c**). All the scale bars are 20 μ m in length, and similar results were obtained in two independent replicates (**a-c**).



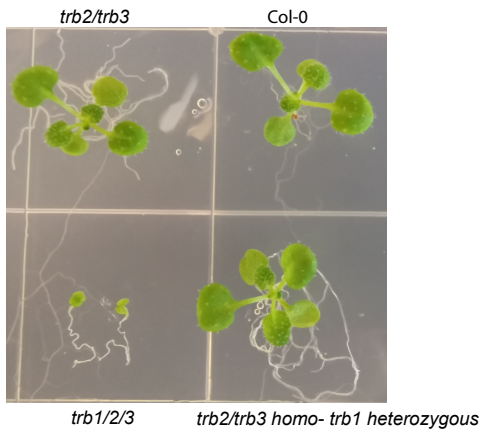
Supplementary Fig. 2 TRBs are partially colocalized with JMJ14, NAC050, and NAC052. a-c Metaplots and heatmaps showing FLAG-TRB1, 2, 3 ChIP-seq signals over FLAG-TRB1 peaks and shuffled peaks (a, n=22,365), FLAG-TRB1 and FLAG-JMJ14 ChIP-seq signals over HA-NAC050 peaks (n=801) and shuffled peaks (b), and HA-NAC050 and HA-NAC052 ChIP-seq signals over the TRB1 Cluster 1 peaks (n=3,089) and the Cluster 2 peaks (n=19,006) (c).



Supplementary Fig. 3 JMJ14 and TRB1 are colocalized at gene body regions. a-c Heatmaps and metaplots representing FLAG-JMJ14 (a), FLAG-TRB1 (b), and H3K4me3 (c) ChIP-seq signals over the TRB1 Cluster 1 proximal genes (n=2,617) and the Cluster 2 proximal genes (n=12,265).



Supplementary Fig. 4 Predicted TRB binding motifs include the telomeric repeat DNA sequence TTAGGG and the known JMJ14 binding motif CTTGnnnnCAAG. a Motif prediction by Homer showing the top 3 binding motifs of TRB1, TRB2, and TRB3. **b** Motif prediction by Homer showing that JMJ14, TRBs, NAC050, and NAC052 are all predicted to bind the TTAGGG and CTTGnnnnCAAG motifs. **c** Pie charts indicate the percentile of the TRB1 and JMJ14 co-bound peaks (top panel) and shuffled peaks (bottom panel) displaying the TTAGGG motif only (n=1,176), the CTTGnnnnCAAG motif only (n=431), both motifs (n=396), and neither (n=1,180), respectively. **d** Heatmaps and metaplots representing the normalized HA-NAC050/052, FLAG-TRB1, FLAG-TRB2, FLAG-TRB3, and FLAG-JMJ14 ChIP-seq signals over TRB1 and JMJ14 co-bound regions displaying the TTAGGG motif only, the CTTGnnnnCAAG motif only, both motifs, and neither, respectively.



trb1/2/3



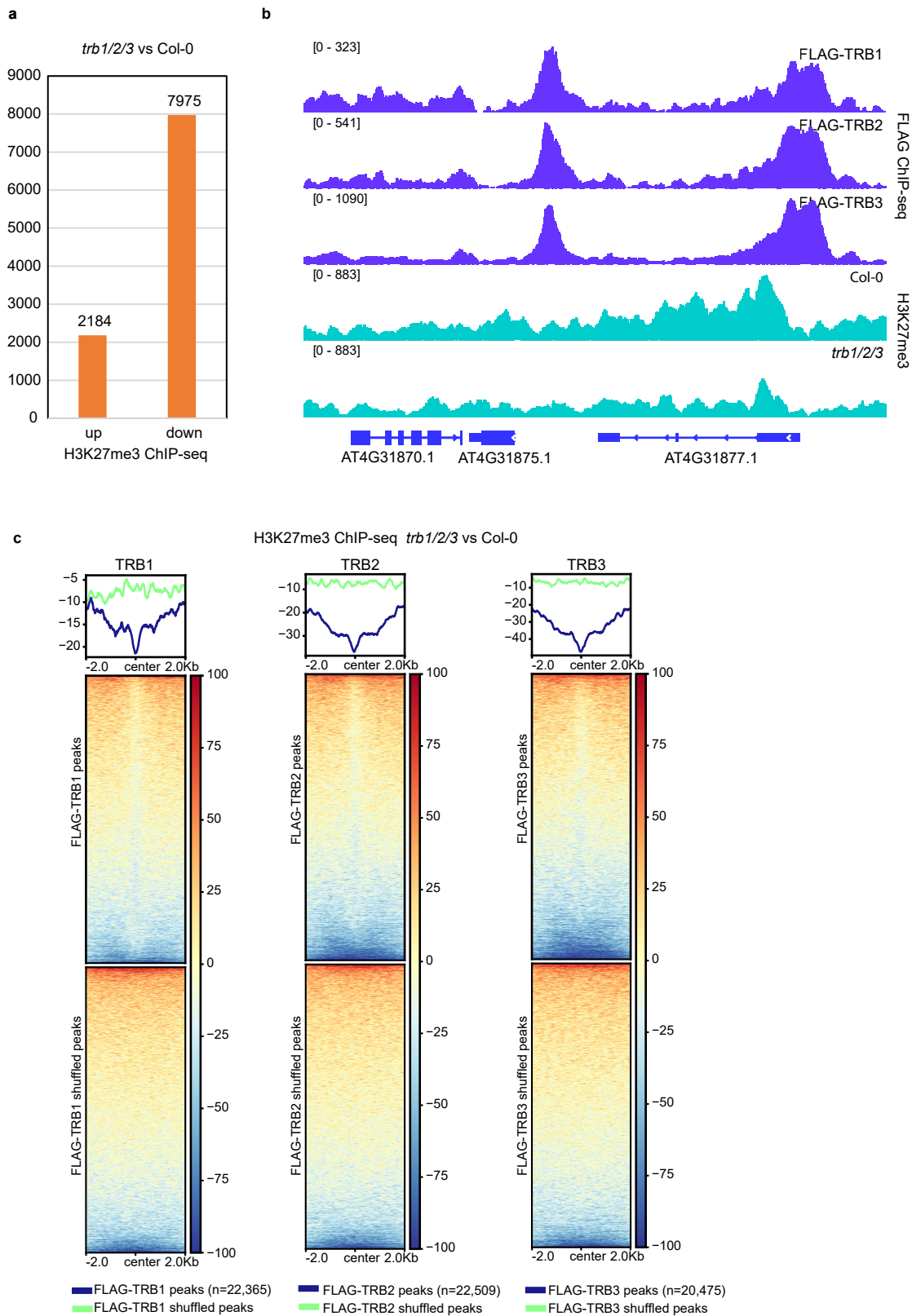
Col-0

trb2/trb3

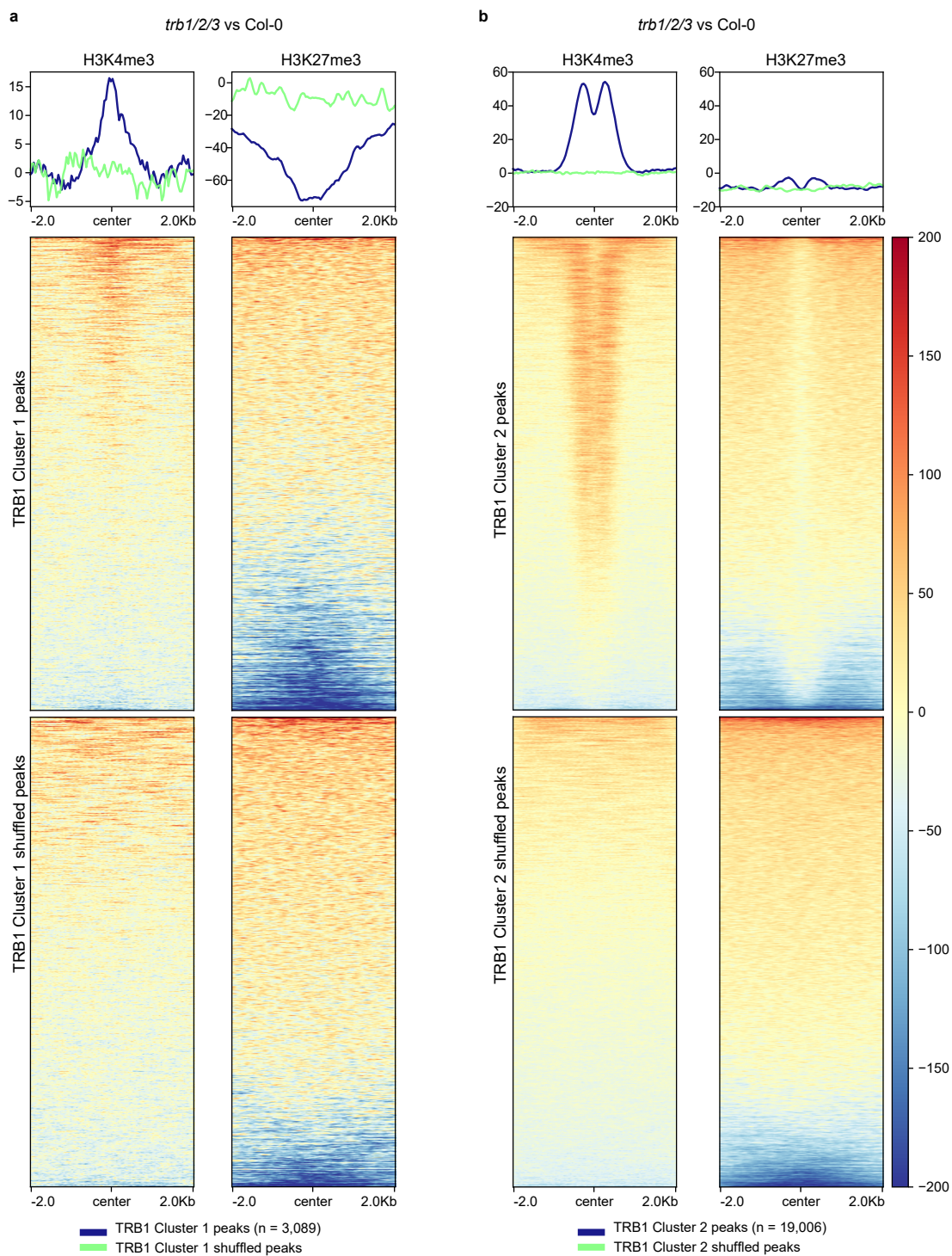
trb2/trb3 homo- *trb1* heterozygous

trb1/2/3

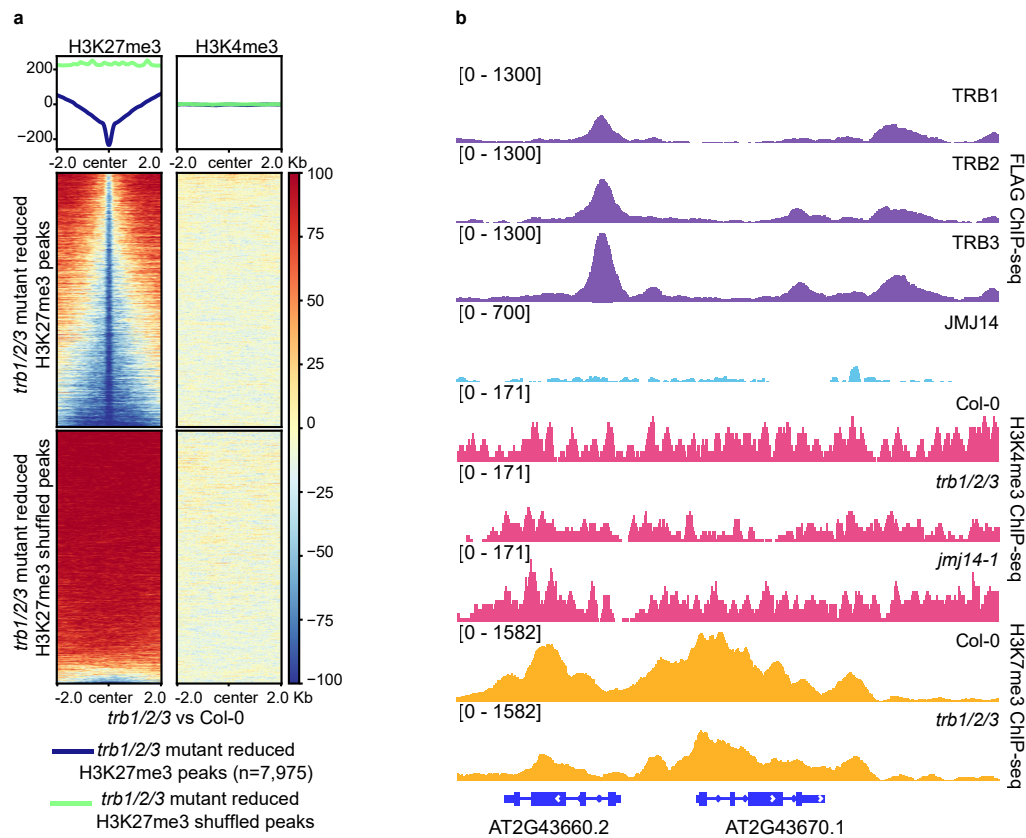
Supplementary Fig. 5 The *trb1/2/3* triple mutant shows strong morphological defects. The photos show the phenotype of *trb2/3* double mutant, Col-0, *trb1/2/3* triple mutant, and *trb2/3* homo- *trb1* heterozygous mutant grown on MS medium for 2-3 weeks (top left), and then transferred to soil for another 2 weeks (bottom). The top right photo shows a closer view of a *trb1/2/3* triple mutant on soil.



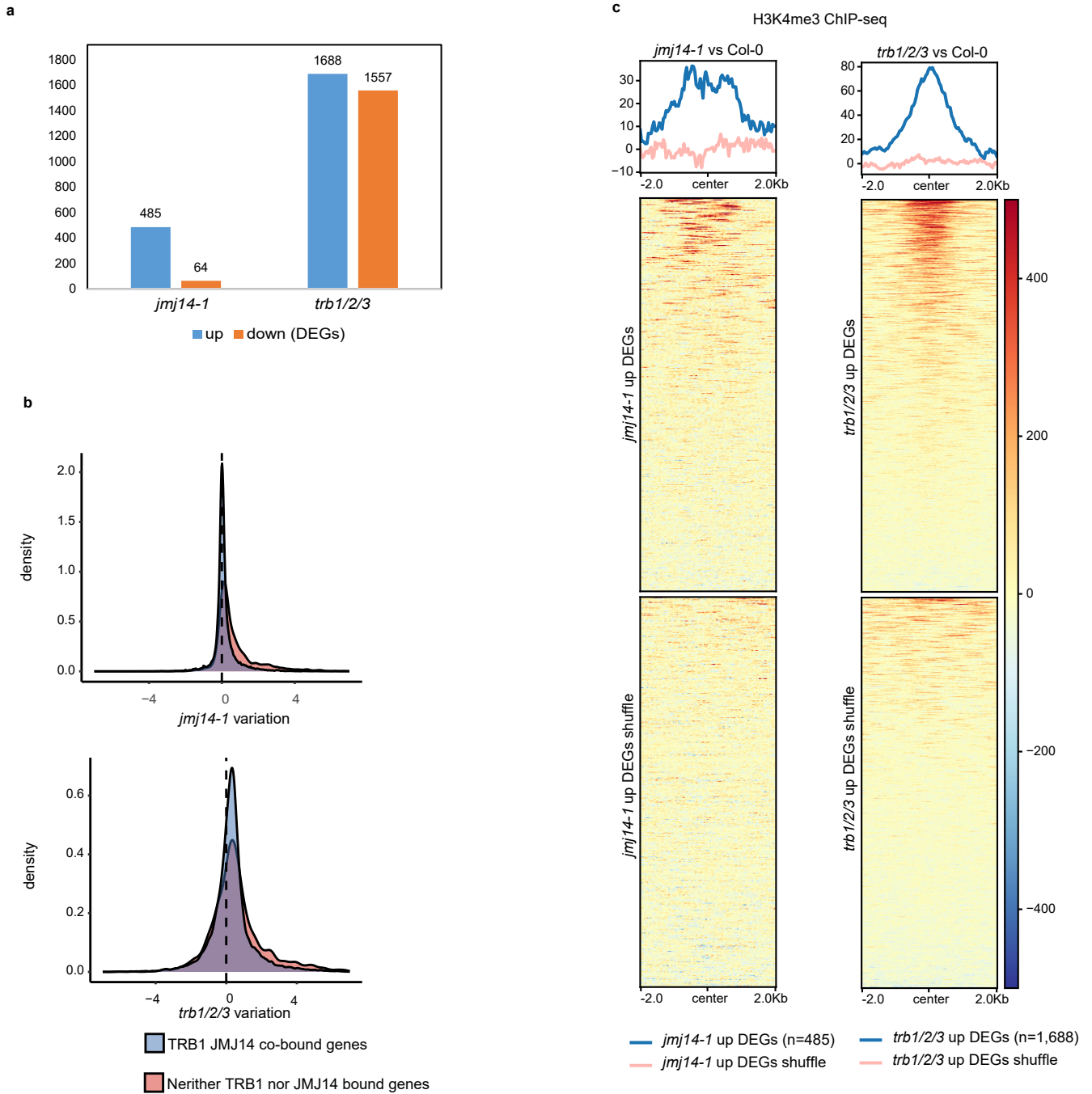
Supplementary Fig. 6 H3K27me3 ChIP-seq signals are reduced in the *trb1/2/3* mutant. **a** Bar chart indicates the number of regions with up- or down-regulated H3K27me3 ChIP-seq signals in the *trb1/2/3* mutant, respectively. **b** Screenshots showing FLAG ChIP-seq signals in FLAG-TRB1, FLAG-TRB2, and FLAG-TRB3 (top three lanes), and H3K27me3 ChIP-seq signals in Col-0 and the *trb1/2/3* mutant, over a representative region. **c** Metaplots and heatmaps representing H3K27me3 ChIP-seq signals in the *trb1/2/3* mutant versus Col-0 wild type over FLAG-TRB1 peaks and shuffled peaks (n=22,365, left panel), FLAG-TRB2 peaks and shuffled peaks (n=22,509, middle panel), and FLAG-TRB3 peaks and shuffled peaks (n=20,475, right panel).

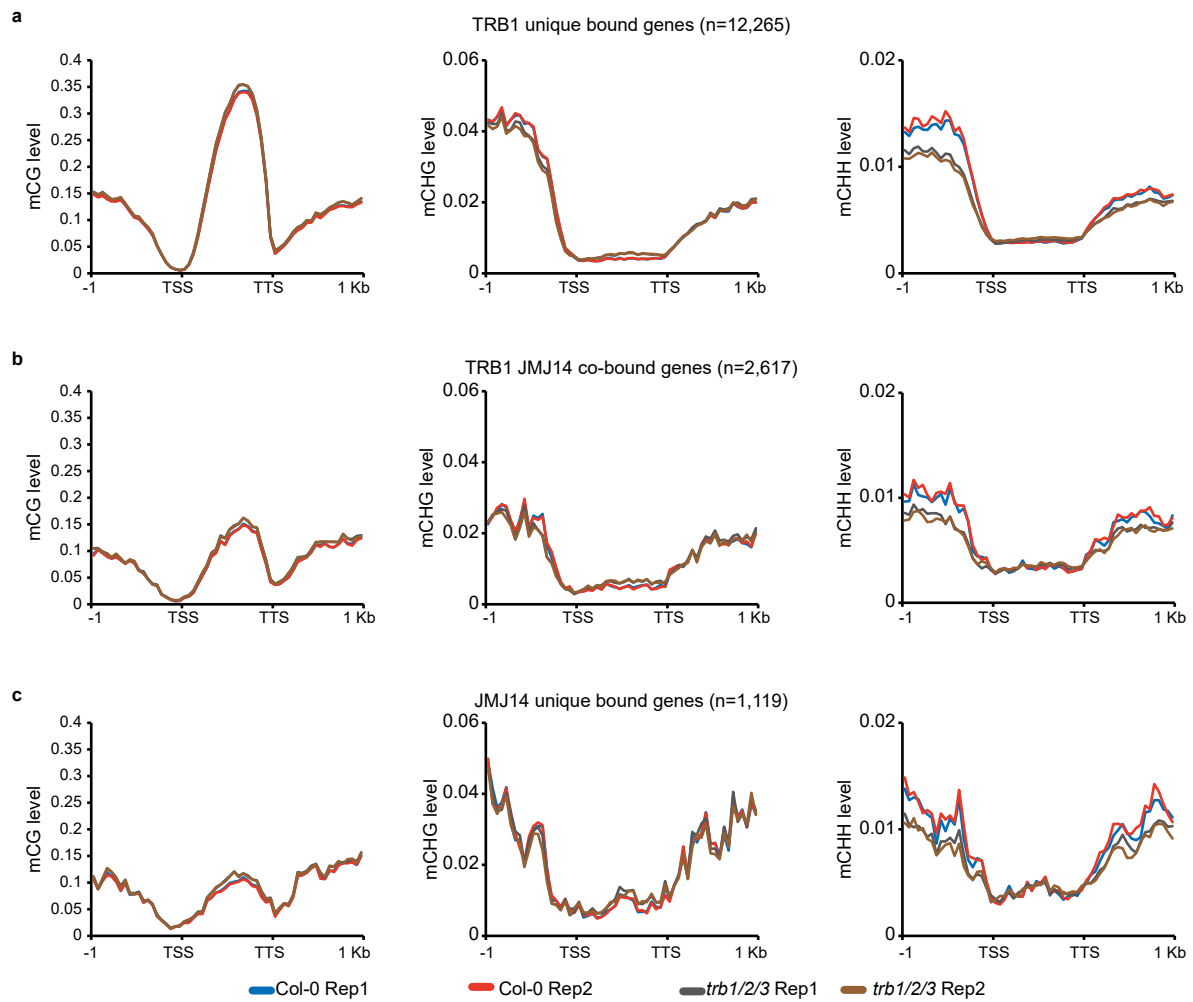


Supplementary Fig. 7 Changes of H3K4me3 and H3K27me3 ChIP-seq signals in the *trb1/2/3* mutant displayed opposite trends at TRB1-JMJ14 co-bound regions. a-b Metaplots and heatmaps depicting the normalized H3K4me3 and H3K27me3 ChIP-seq signals in the *trb1/2/3* mutant versus Col-0 at TRB1 Cluster 1 peaks and shuffled peaks (a, n=3,089), and TRB1 Cluster 2 peaks and shuffled peaks (b, n=19,006), respectively.

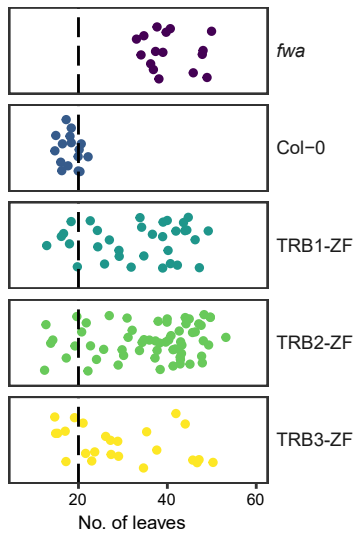
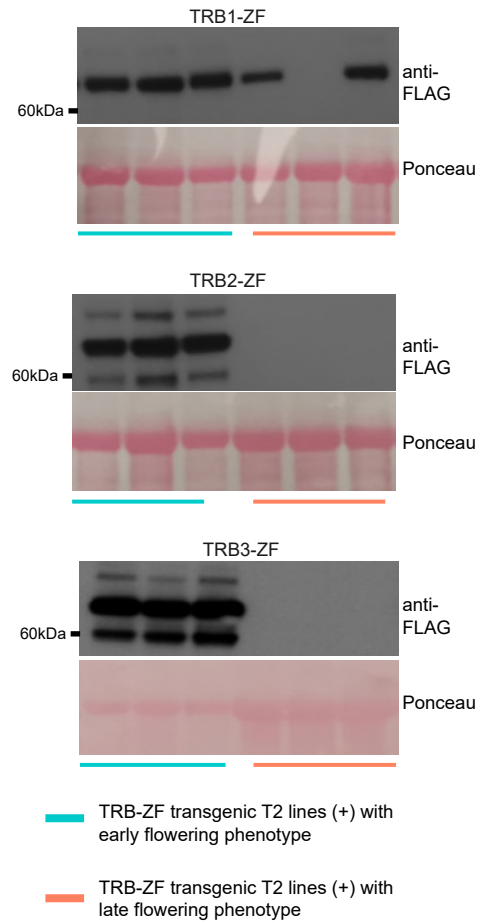


Supplementary Fig. 8 The reduction of H3K27me3 does not always trigger an increase of H3K4me3 in the *trb1/2/3* mutant. **a** Metaplots and heatmaps depicting H3K27me3 and H3K4me3 ChIP-seq signals over the reduced H3K27me3 peaks and shuffled peaks (n=7,975) in the *trb1/2/3* mutants versus Col-0 wild type. **b** Screenshots showing FLAG ChIP-seq signals of FLAG-TRB1, FLAG-TRB2, FLAG-TRB3, and FLAG-JMJ14, H3K4me3 ChIP-seq signals in Col-0, *trb1/2/3*, and *jmj14-1* mutants, and H3K27me3 ChIP-seq signals in Col-0 and the *trb1/2/3* mutant over a representative region.

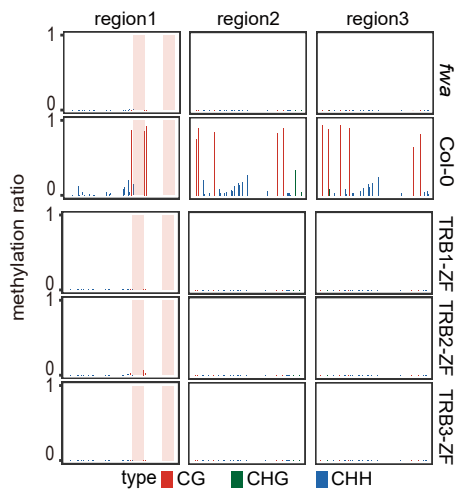
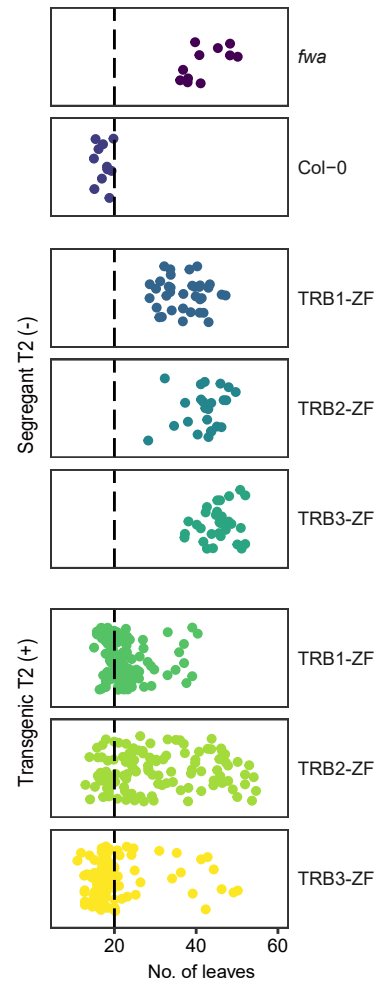




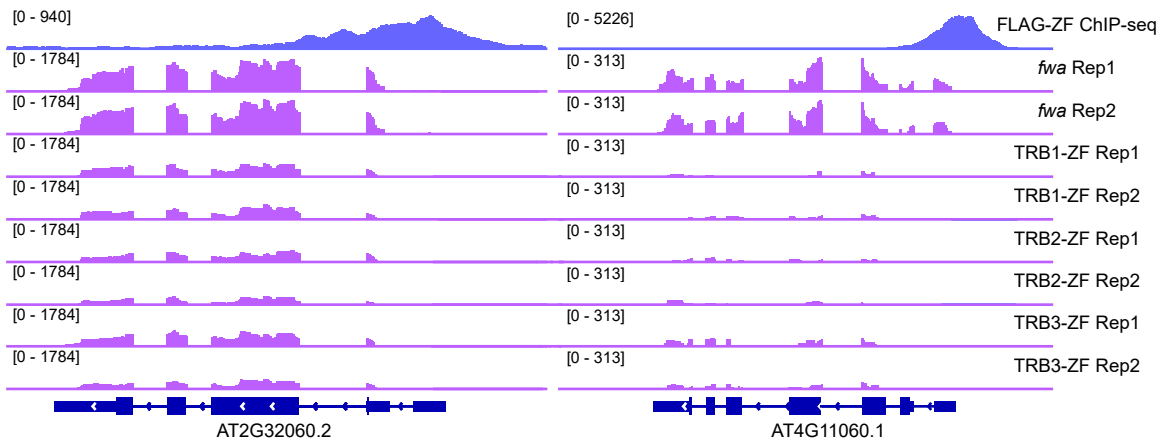
Supplementary Fig. 10 CHH DNA methylation level is reduced in the *trb1/2/3* mutant. a-c CG, CHG, and CHH DNA methylation levels in two replicates of Col-0 and *trb1/2/3* triple mutants over 1 kb flanks of TRB1 unique bound genes (**a**, n=12,265), TRB1-JMJ14 co-bound genes (**b**, n=2,617), and JMJ14 unique bound genes (**c**, n=1,119). The DNA methylation levels were measured by whole genome bisulfite sequencing.

a**b**

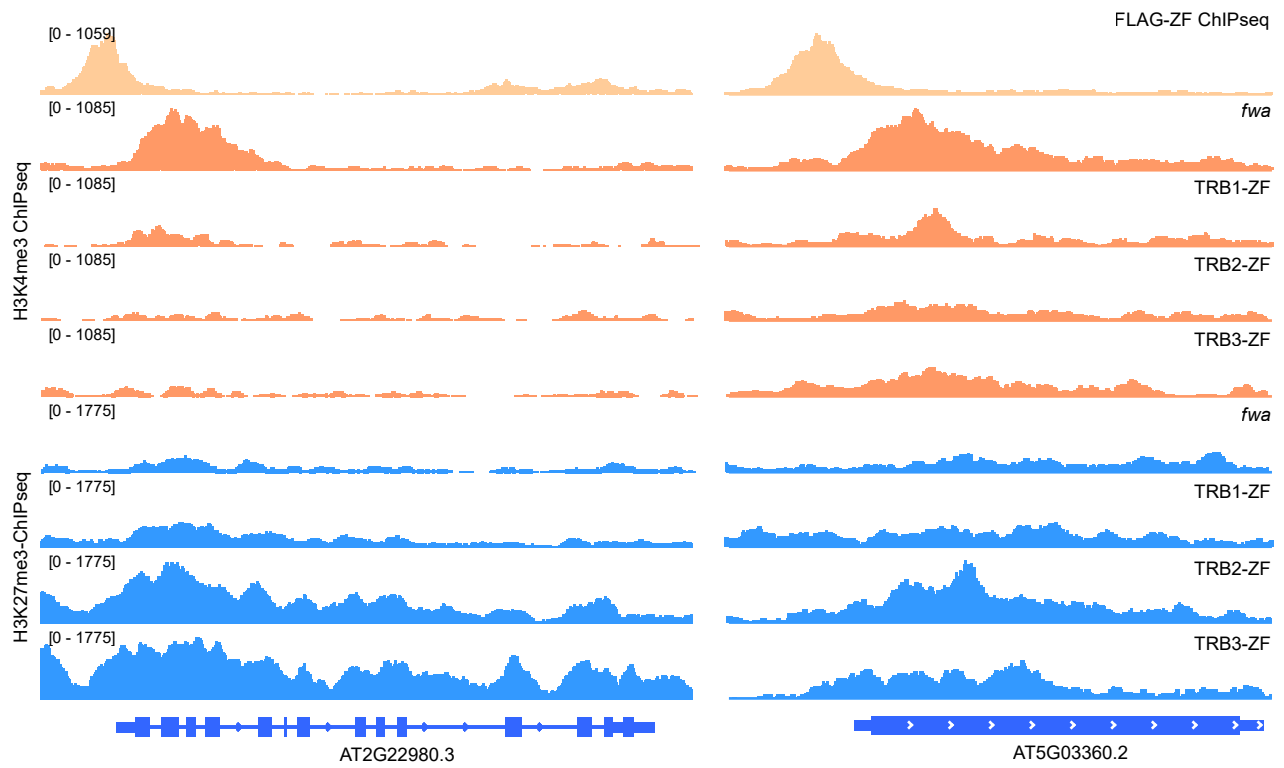
Supplementary Fig. 11 TRB-ZF T1 lines restore an early flowering phenotype in *fwa*. **a** Dot plots showing the leaf count of *fwa*, Col-0, and the T1 lines of TRB1-ZF, TRB2-ZF, and TRB3-ZF. **b** Western blot of the TRB-ZF fusions in T2 transgenic lines showing early flowering phenotypes (left three samples) and late flowering phenotypes (right three samples), respectively. Similar results were observed in two biological replicates.

a**b**

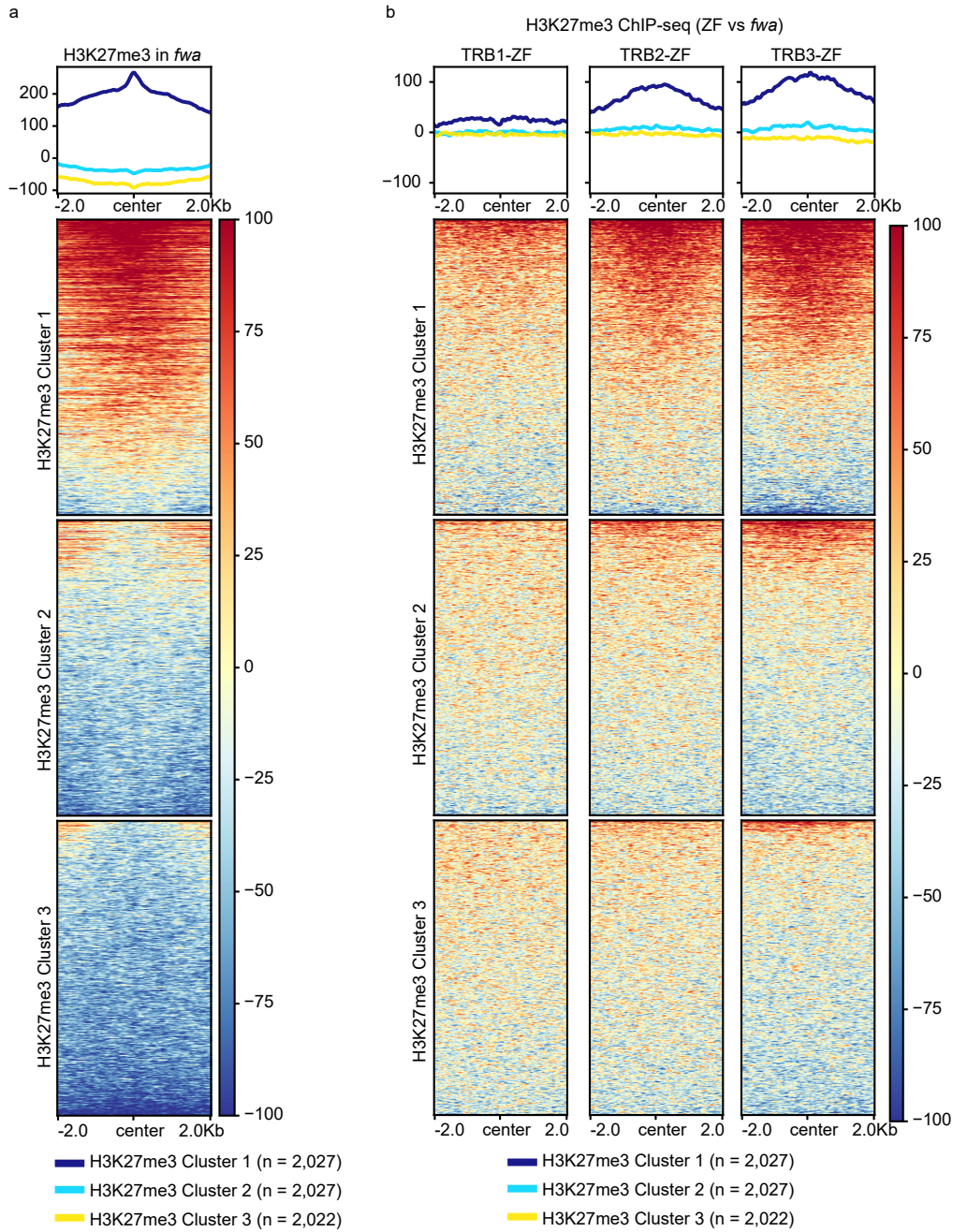
Supplementary Fig. 12 The TRB-ZF fusions triggered early flowering phenotype is not associated with DNA methylation and is not heritable in T2 null segregant lines. a CG, CHG, and CHH DNA methylation level over *FWA* promoter regions measured by bisulfite PCR-seq. Pink vertical boxes indicate ZF binding sites. **b** Dot plots represent the leaf counts of *fwa*, Col-0, null segregant and transgenic T2 lines of TRB1-ZF, TRB2-ZF, and TRB3-ZF, respectively.



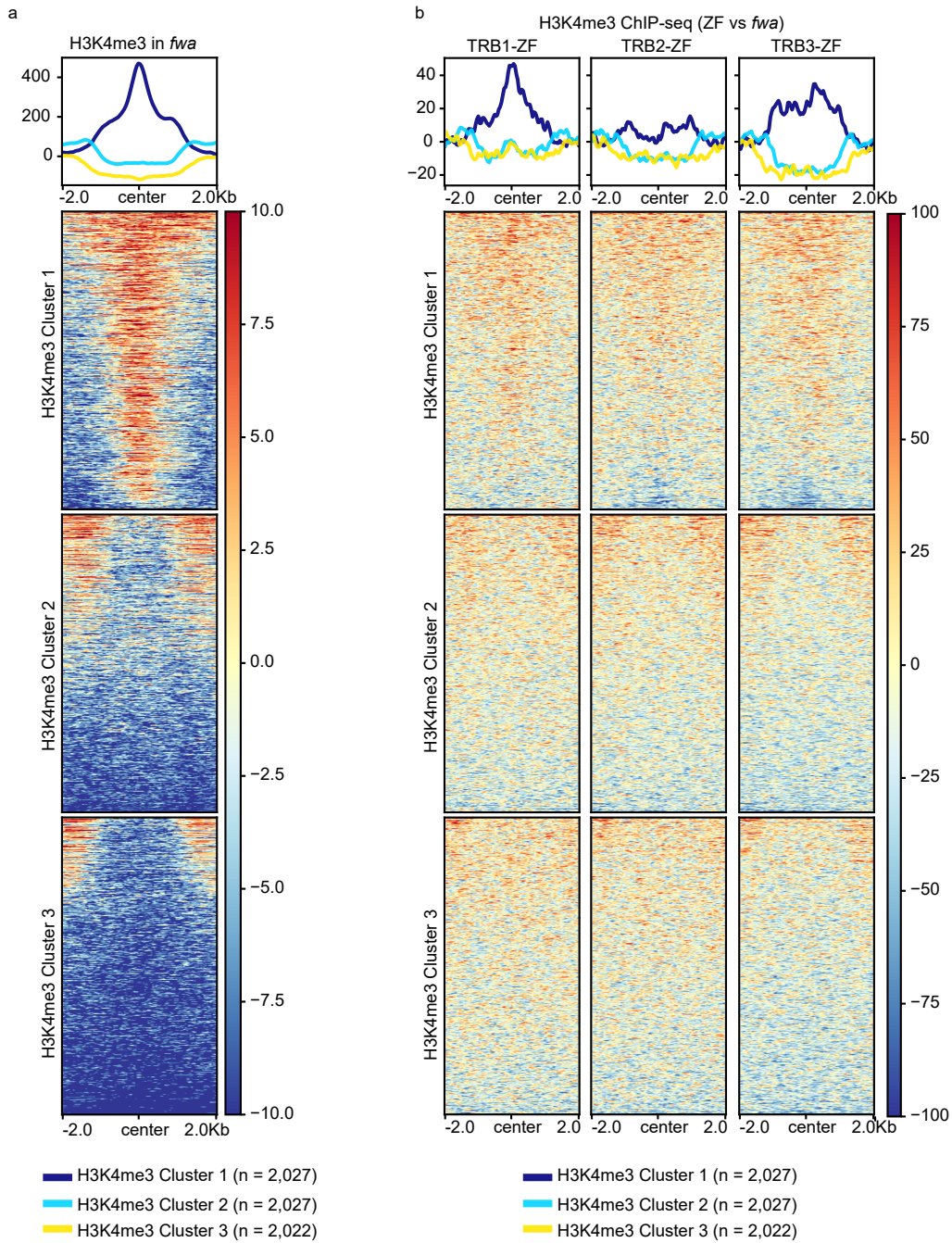
Supplementary Fig. 13 TRB-ZF fusions triggered gene silencing over two representative ZF off-target sites. Screenshots showing two replicates of RNA-seq signals in *fwa*, TRB1-ZF, TRB2-ZF, and TRB3-ZF over two representative ZF off target sites. FLAG-ZF ChIP-seq indicates the ZF binding sites.



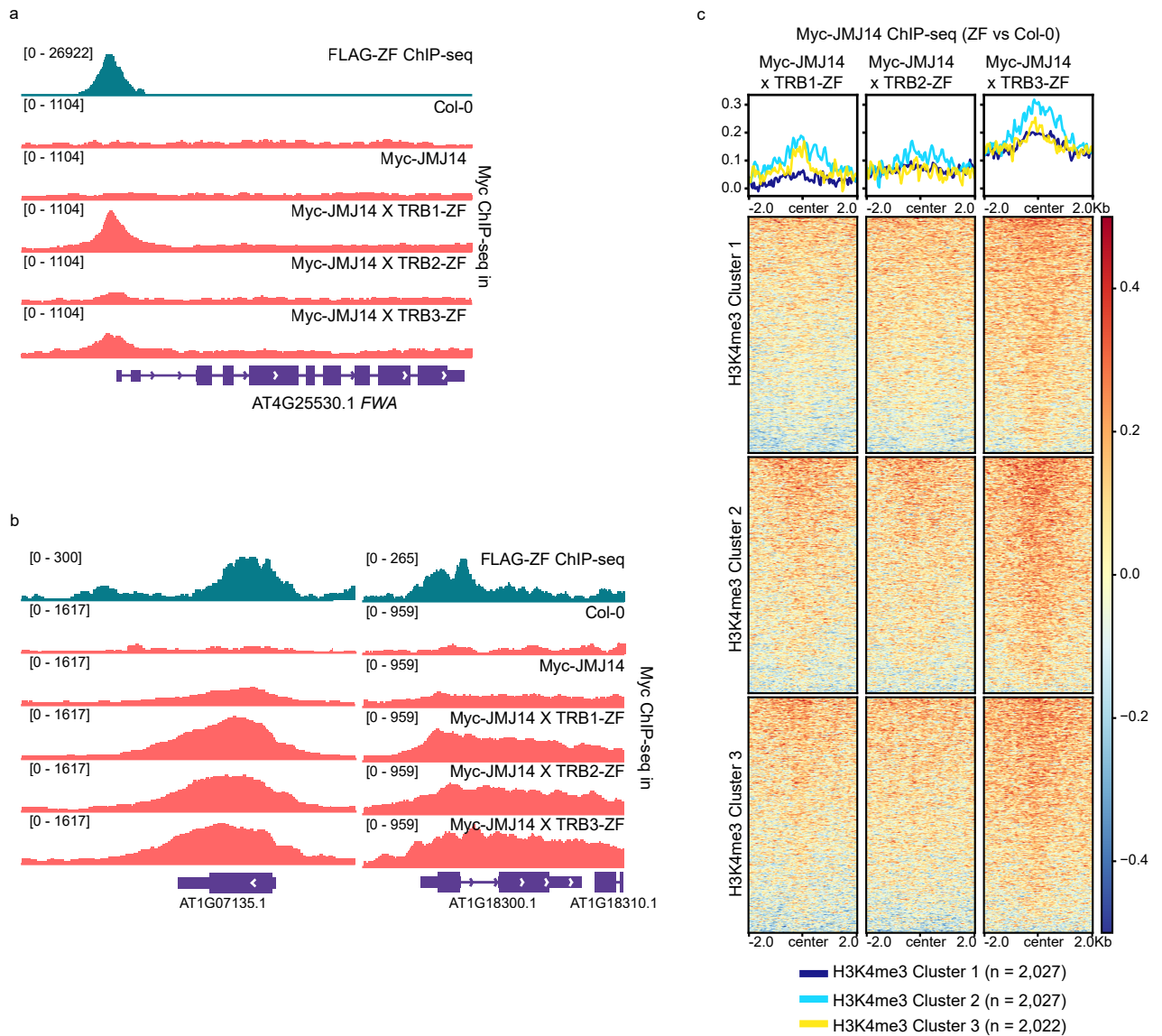
Supplementary Fig. 14 TRB-ZF fusions triggered H3K4me3 demethylation and H3K27me3 deposition over two representative ZF off-target sites. Screenshots of H3K4me3 and H3K27me3 ChIP-seq signals in *fwa*, TRB1-ZF, TRB2-ZF, and TRB3-ZF over two representative ZF off target sites. FLAG-ZF ChIP-seq indicates the ZF binding sites.



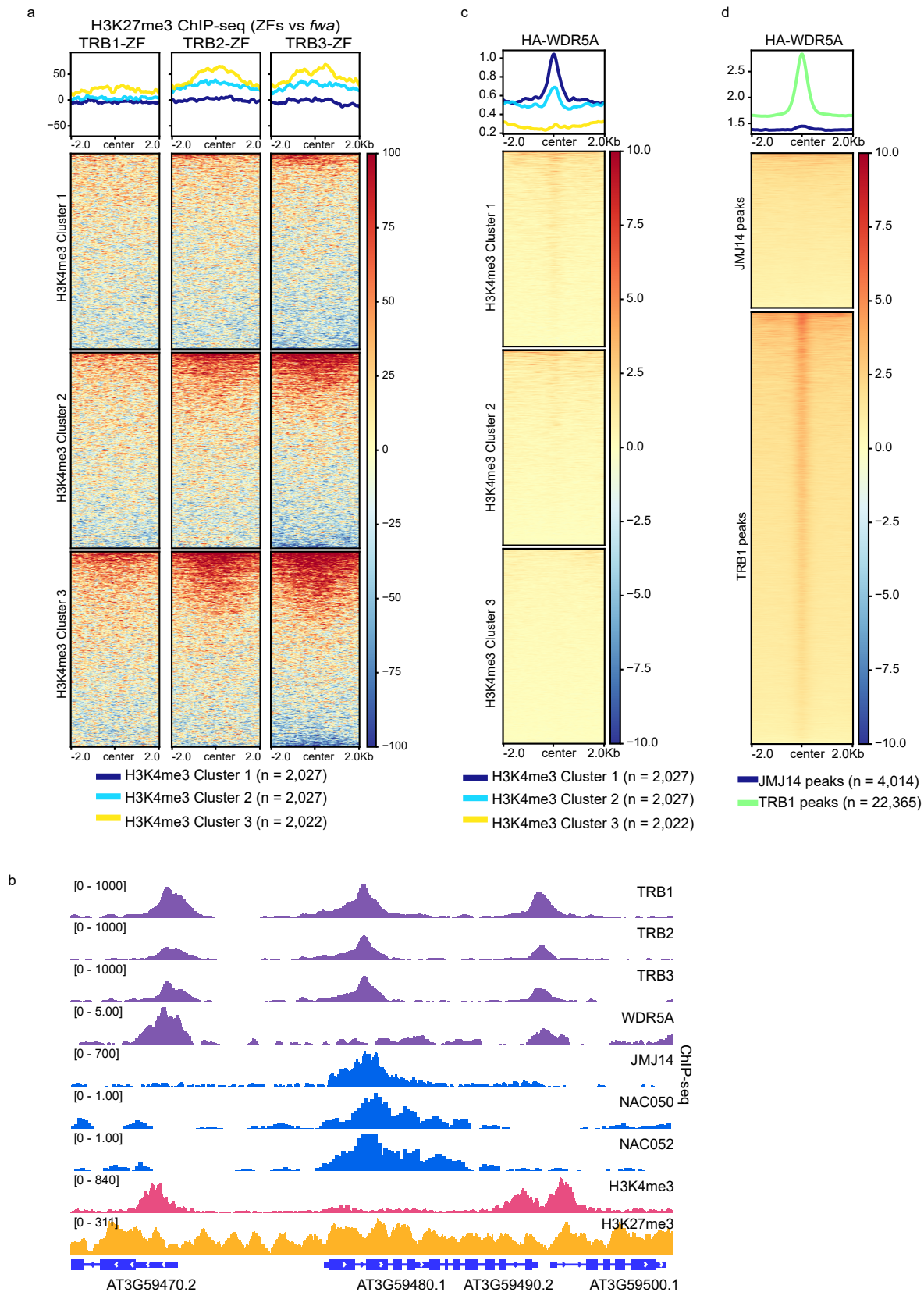
Supplementary Fig. 15 TRB-ZFs triggered H3K27me3 deposition mainly occurs at ZF off-target sites with high levels of pre-existing H3K27me3. a Metaplot and heatmaps representing the normalized H3K27me3 ChIP-seq signals in *fwa* plant over three clusters of ZF off-target sites with high (H3K27me3 Cluster1, n=2,027), medium (H3K27me3 Cluster2, n=2,027), or low (H3K27me3 Cluster3, n=2,022) levels of pre-existing H3K27me3. **b** Metaplots and heatmaps showing the normalized H3K27me3 ChIP-seq signals in TRB-ZFs versus *fwa* over three H3K27me3 clusters.



Supplementary Fig. 16 TRB-ZFs triggered H3K4me3 removal mainly occurs at ZF off-target sites with medium or low levels of pre-existing H3K4me3. a Metaplots and heatmaps showing the normalized H3K4me3 ChIP-seq signals in *fwa* over three clusters of ZF off-target sites with high (H3K4me3 Cluster1, n=2,027), medium (H3K4me3 Cluster2, n=2,027), or low (H3K4me3 Cluster3, n=2,022) levels of pre-existing H3K4me3. **b** Metaplots and heatmaps showing the normalized H3K4me3 ChIP-seq signals in TRB-ZFs versus *fwa* over the three H3K4me3 clusters.



Supplementary Fig. 17 The recruitment of JMJ14 by TRB-ZFs mainly occurs at the ZF off-target sites with medium or low levels of pre-existing H3K4me3. a-b Screenshots of Myc ChIP-seq in Col-0 plant, Myc-JMJ14 transgenic lines in Col-0, TRB1-ZF, TRB2-ZF, and TRB3-ZF backgrounds at *FWA* (a) and two representative ZF off-target genes (b). FLAG-ZF ChIP-seq indicates the ZF binding site. **c** Normalized Myc-JMJ14 ChIP-seq signals over three H3K4me3 Clusters of ZF off-target sites in Myc-JMJ14 x TRB-ZFs crossed lines versus Myc-JMJ14 transgenic line in Col-0 background.



Supplementary Fig. 18 TRB-ZF might recruit WDR5A to add H3K4me3 to ZF off-target sites with high levels of pre-existing H3K4me3. **a** H3K27me3 ChIP-seq in TRB-ZFs versus *fwa* over three H3K4me3 clusters of ZF off-target sites. **b** Screenshots representing the ChIP-seq of FLAG-TRB1, FLAG-TRB2, FLAG-TRB3, FLAG-JMJ14, HA-WDR5A, HA-NAC050, HA-NAC052, H3K4me3, and H3K27me3 over a representative locus. **c-d** Metaplots and heatmaps depicting HA-WDR5A ChIP-seq signals over three H3K4me3 clusters of ZF off-target sites (**c**), or over JMJ14 peaks (n=4,014) or TRB1 peaks (n=22,36) (**d**).